ELSEVIER

Journal of Molecular Catalysis A: Chemical 182–183 (2002) 489–498

JOURNAL OF MOLECULAR CATALYSIS A: CHEMICAL

www.elsevier.com/locate/molcata

The role of protons in hydroamination reactions involving homogeneous and heterogeneous catalysts

J. Penzien, R.Q. Su, T.E. Müller*

Institut für Technische Chemie II, Technische Universität München, Lichtenbergstraße 4, 85747 Garching, Germany

Received 28 August 2001; accepted 11 October 2001

Abstract

The addition of amines to CC double and triple bonds using different transition metal catalysts was investigated. Lewis acidic complexes of rhodium, palladium, copper and zinc are effective catalysts for the cyclisation of 3-aminopropyl-vinylether and 6-aminohex-1-yne. The catalytic activity of these homogeneous catalysts is significantly increased in the presence of catalytic amounts of Brønsted acids. The higher activity of corresponding heterogeneous catalysts, here shown for zinc ion exchanged beta zeolites, is probably related to residual protons in the material. The respective role played by Lewis acidic metal centres and protons in the catalytic systems is discussed. It is concluded that Brønsted and Lewis acids, and their respective properties, have to be taken into account in the rational design of hydroamination processes mediated by late transition metals.

Keywords: Hydroamination; Addition; Amine; Alkyne; Alkene

1. Introduction

Amines are important chemical intermediates which have applications, e.g., in the synthesis of polymers, various solvents, pharmaceuticals and surfactants. The chemical industry produces amines in small to medium scale facilities utilising various synthetic routes [1]. Currently, the most widespread method for the production of lower alkyl amines involves the reaction of an alcohol with ammonia. A major drawback of this route is that (i) water is formed in the reaction which has to be separated from the product amine and (ii) the alcohol is frequently obtained by direct or indirect hydration of the corresponding alkene. The direct addition of amines to carbon–carbon multiple bonds (hydroamination) would save at least one step in commercial operations and, therefore, faces increasing attention as an atom efficient catalytic transformation.

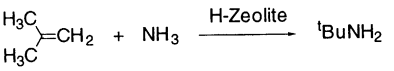

(1)

So far, most studies have been focused on the reaction between ammonia and C2–C4 alkenes. The amination of 2-methylpropene, e.g., gives *t*-butylamine (Eq. (1)) [2–4]. The reaction is slightly exothermic and has a negative reaction entropy [5]. Therefore, the thermodynamic equilibrium is shifted to the starting materials and the yield decreases with increasing temperature (Fig. 1) [6]. Because of the low reactivity of the two reactants, a catalyst is required. Most commonly, solid acids and especially zeolites in the protonic form are used. Since 1986, BASF AG have operated an industrial scale process for the production of *t*-butylamine [7]. The reaction is

* Corresponding author. Tel.: +49-89-289-13538; fax: +49-89-289-13544.
E-mail address: thomas.mueller@ch.tum.de (T.E. Müller).

1381-1169/02/$ – see front matter
PII: S1381-1169(01)00496-4

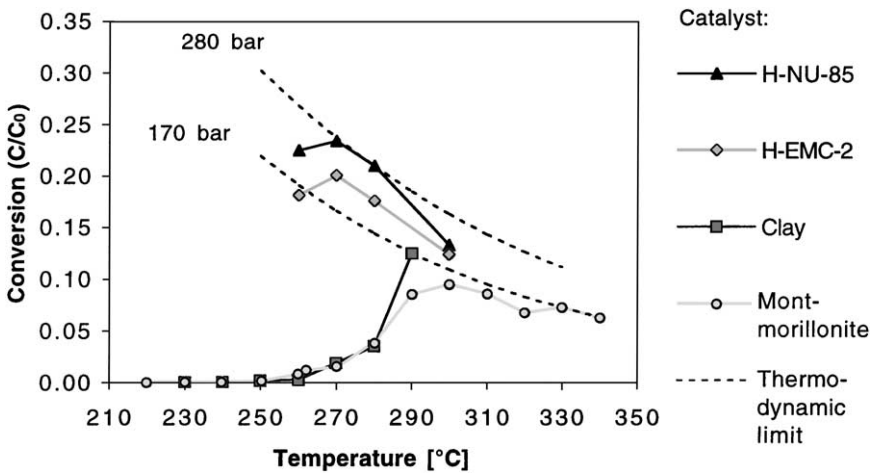

Fig. 1. Dependence of the conversion of 2-methylpropene to *t*-butylamine on the reaction conditions, i.e., the temperature, pressure and catalyst [6].

performed at approximately 270 °C and 280 bar, i.e., at supercritical conditions, using a fixed bed catalyst [8]. The maximum conversion of ca. 24% at this temperature makes recyclisation of 2-methylpropene and ammonia necessary, which is a costly factor in the commercial operation.

Catalysis of hydroamination reactions with solid acids is restricted to those alkenes, which form relatively stable alkoxy groups. A new type of catalyst was required which was able to activate the alkene in a different manner. Thus, we explored the use of late transition metal catalysts. In this study, complexes of late transition metals and ion exchanged zeolites have been shown to be excellent catalysts for the intramolecular hydroamination of alkenes and alkynes. In particular, the cyclisation of 3-aminopropyl-vinylether and 6-aminohex-1-yne with these catalysts was explored. Here, the role of Lewis and Brønsted acids as catalytically active sites is discussed in light of the analogy between homogeneous and heterogeneous catalysis.

2. Experimental

^{1}H, and $^{31}P\{^{1}H\}$-NMR spectra were recorded on a Bruker AM 400 spectrometer. Chemical shifts are reported in ppm relative to tetramethylsilane. Analytical gas chromatography was performed on a Hewlett-Packard HP 5890 gas chromatograph with a flame ionisation detector, using a crosslinked 5% diphenyl- 95% dimethyl-polysiloxane column (30 m, Restek GmbH, Rtx-5 Amine). 6-Aminohex-1-yne and $[Pd(Triphos)](CF_3SO_3)_2$ were prepared according to the published procedures [9]. All other chemicals were commercially obtained and used as received; CH_3CN and toluene were purchased anhydrous from Aldrich. Zinc ion-exchanged zeolites were prepared by slurring the H-beta zeolite (Südchemie AG, T-4546, MA039 H/99, specific surface area 536 m^2/g, 10 g) with 0.5 M zinc acetate in water (70 cm^3) at 80 °C and separated subsequently by centrifuging the mixture. The procedure was repeated four times to ensure complete ion-exchange. Finally, the sample was calcined (5 K/min to 500 °C, 4 h at 500 °C). To achieve lower degrees of ion-exchange a less concentrated zinc acetate solution was used and the procedure was repeated less often. The zinc loadings were determined by atomic absorption spectroscopy (0.03–0.66 mmol Zn^{2+}/g).

In a typical catalytic experiment, a mixture of 6-aminohex-1-yne (0.06 cm^3, 0.5 mmol), zinc exchanged beta zeolite (11 mg) and toluene (15 cm^3) was heated at reflux (111 C) and samples taken for GC analysis at regular intervals. In the comparison of different homogenous catalysts, the same reaction conditions and the following amounts of catalyst (5.3×10^{-3} mmol) and acid were employed: 2.4 mg $[Rh(NOR)_2]ClO_4$, 4.8 mg $[Pd(Triphos)](CF_3SO_3)_2$,

2.0 mg $[Cu(CH_3CN)_4]PF_6$ or 1.9 mg $Zn(CF_3SO_3)_2$; 0, 4.7×10^{-4}, 2.3×10^{-3}, 4.7×10^{-3} cm^3 CF_3SO_3H (0, 5.3×10^{-3}, 2.1×10^{-2}, 5.3×10^{-2} mmol, respectively). In the cyclisation of 3-aminopropyl-vinylether, a mixture of the substrate (0.1 cm^3, 0.9 mmol), catalyst (4.4×10^{-2} mmol) and toluene (15 cm^3) was heated at reflux (111 °C). The acid CF_3SO_3H was added within of the first 2 min of the reaction. Samples for GC analysis were then taken at regular intervals. For the experiments the following amounts of catalyst and acid were used: 21 mg $[Rh(NOR)_2]ClO_4$, 42 mg $[Pd(Triphos)](CF_3SO_3)_2$, 17 mg $[Cu(CH_3CN)_4PF_6$ or 16 mg $Zn(CF_3SO_3)_2$; 0, 3.9×10^{-3}, 1.9×10^{-2}, 3.9×10^{-2} cm^3 CF_3SO_3H (0, 4.4×10^{-2}, 2.2×10^{-1}, 4.4×10^{-1} mmol, respectively).

The reactions involving optical spectroscopy were carried out in a custom built 90 cm^3 steel autoclave equipped with two pairs of movable quartz probes [10]. The probes were connected with optical fibres to a Perkin Elmer Lambda 16 UV spectrometer and a Bruker Vector 22/N NIR spectrometer, respectively. The spectra obtained were baseline corrected and then integrated in the frequency range 4830–5070 cm^{-1} (NIR, characteristic for **3**) and 220–370 nm (UV, characteristic for **5**). For the in situ NIR/UV experiment, the initial reaction mixture contained 6-aminohex-1-yne (0.17 cm^3, 1.5 mmol), $[Pd(Triphos)](CF_3SO_3)_2$ (14.2 mg, 15 μmol) and CH_3CN (60 cm^3) at 82 °C. For the comparison between homogeneous and heterogeneous catalysis, the reaction mixtures contained: (a) 6-aminohex-1-yne (0.28 cm^3, 2.5 mmol), $Zn(CF_3SO_3)_2$ (9.2 mg, 25 μmol) in toluene (60 cm^3); (b) 6-aminohex-1-yne (0.32 cm^3, 2.8 mmol), $Zn(CF_3SO_3)_2$ (10.3 mg, 28 μmol) and CF_3SO_3H (0.05 cm^3, 0.56 mmol) in toluene (60 cm^3) and (c) 6-aminohex-1-yne (0.26 cm^3, 2.4 mmol), Zn–H-beta (48 mg, 23 μmol Zn^{2+}) in toluene (60 cm^3) at 111 °C.

3. Results and discussion

The cyclisation of 3-aminopropyl-vinylether (**1**), which allows for a slightly activated carbon–carbon double bond, gives N,O-acetal tetrahydro-2-methyl-1,3-oxazine (**2**) (Eq. (2)). The intramolecular hydroamination of 6-aminohex-1-yne (**3**) first generates 2-methylene-piperidine (**4**) with an exocyclic double bond which isomerises in situ to the more stable imine 2-methyl-1,2-dehydropiperidine (**5**) (Eq. (3)).

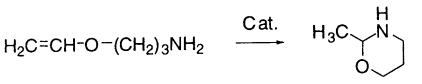

1 2 (2)

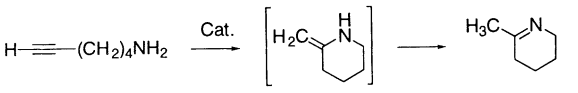

3 4 5 (3)

As homogeneous catalyst, the palladium complex $[Pd(Triphos)](CF_3SO_3)_2$ (**6**) was studied in detail. Complex **6** was prepared from $[PdCl_2(COD)]$ by displacement of the COD ligand by the phosphine ligand followed by halide abstraction with $AgCF_3SO_3$. The nature of **6** was confirmed by single crystal X-ray analysis [11]. Suitable crystals of **6**·$CHCl_3$ were grown by slow evaporation of a chloroform solution of complex **6**. A perspective view of the monocationic part of the complex is shown in Fig. 2. The phosphine is coordinated in a three-dentate fashion to the palladium centre. The anticipated vacant coordination site *trans* to the PPh phosphorus atom is occupied by an oxygen atom (O1) of one trifluoromethylsulfonate anion. Thus, the geometry is based on the normal square-planar geometry of Pd^{II} centres.

As the counter ion has to be displaced during catalysis, a large influence of the anion on the catalytic activity is expected. In this respect, it was shown that anions, derived from the sulfonic acids, were particularly favourable for a high catalytic activity [9]. In **6**, the strong *trans*-effect of phosphorus labilises the bond to the anion or—during catalysis—to the substrate, intermediate or product. This is probably the reason for the higher catalytic activity of **6** in comparison to palladium complexes where a nitrogen atom is located trans to the empty coordination site [11]. The tridentate phosphine ligand used in this study inevitably makes the oxidative addition of H–N more difficult in comparison to bi- or mono-dentate ligands. Accordingly, the mechanism proposed below is not necessarily applicable to reactions involving palladium complexes with bi- and mono-dentate ligands [12,13].

To obtain kinetic data on the cyclisation of 6-aminohex-1-yne with $[Pd(Triphos)](CF_3SO_3)_2$, the

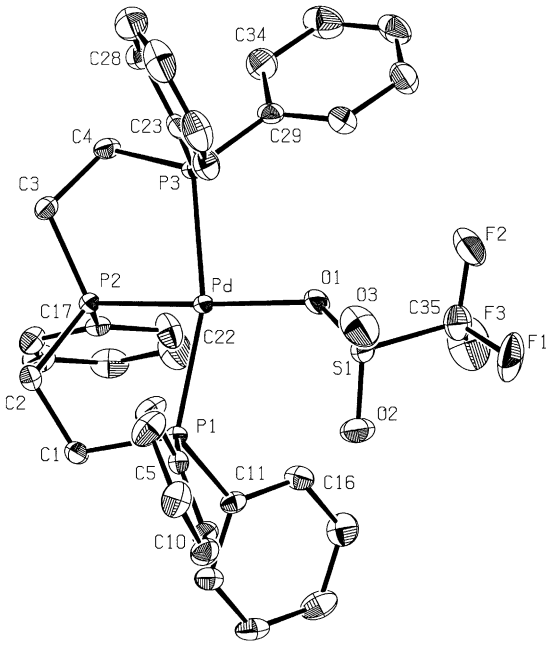

Fig. 2. ORTEP representation of the monocationic part of compound **6**·$CHCl_3$ in the solid state. Thermal ellipsoids are at the 50% probability level. Hydrogen atoms are omitted for clarity. Selected distances (Å) and angles (°): Pd–P1, 2.3375(6); Pd–P2, 2.2003(6); Pd–P3, 2.3480(6); Pd–O1, 2.134(2); P1–Pd–P2, 82.38(2); P1–Pd–P3, 164.14(2); P1–Pd–O1, 99.88(6); P2–Pd–P3, 83.92(2); P2–Pd–O1, 175.48(7); P3–Pd–O1, 94.36(6); Pd–O1–S, 135.82(12) [11].

reaction was followed in situ with optical spectroscopy [14]. Acetonitrile was chosen as solvent, as it has a large spectroscopic window for UV and NIR spectroscopy. The concentrations of the substrate **3** and product **5** were derived from the respective spectra in the NIR and UV region. Initially, the concentration of **3** decreased rapidly, whereas very little amounts of **5** formed (Fig. 3). At longer reaction times, the concentration of **5** increased, but remained always lower than the amount expected from the decrease in **3**. The mass balance could, however, be closed by assuming that an intermediate species had formed. To determine the nature of the intermediate, the reaction was also followed by in situ ^{1}H-NMR spectroscopy. The spectra showed transient signals at 3.40 and 3.24 ppm which were assigned to the methylene group of enamine **4**.

The change in the substrate and product concentration with time could be described by a kinetic model

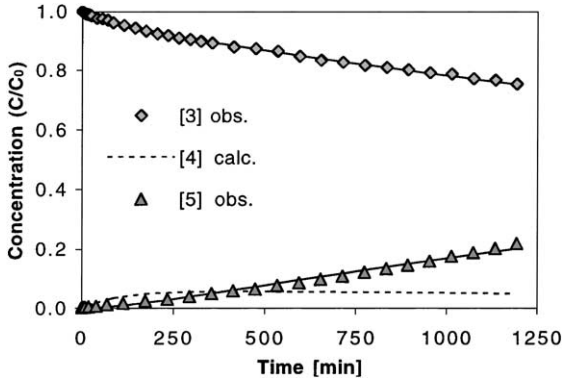

Fig. 3. Concentrations of **3** and **5** in the cyclisation of **3** with $[Pd(Triphos)](CF_3SO_3)_2$ (solvent CH_3CN, 82 °C). The concentrations were followed in situ with NIR and UV spectroscopy, respectively.

based on an equilibrium reaction between **3** and **4**, followed by an effectively irreversible isomerisation of **4**–**5** (Eq. (4)) [14]. From fitting of the corresponding rate equations [15,16], the rate constants $k_1 = 0.54 \times 10^{-3}$, $k_{-1} = 5.06 \times 10^{-3}$ and $k_2 = 3.37 \times 10^{-3}\,\mathrm{min}^{-1}$ were obtained (82 °C). Whereas k_2 describes an elementary reaction, k_1 and k_{-1} constitute formal rate constants describing the overall rate of reaction for the sequence of reaction steps leading from **3** to **4** and the reverse reaction, respectively. The slowest step in the reaction sequence is the formation of intermediate **4**. The intermediate can then react back to the starting material or forward to give the product **5**. Although both reactions are faster than the formation of **4**, the difference in rate does not exceed one order of magnitude. As a consequence, the intermediate reaches a maximum concentration of about 5% after 350 min. The corresponding constant K_{eq} for the equilibrium between **3** and **4** is, therefore, on the side of the starting material ($K_{eq} \approx 0.11$). This value is for the dynamic equilibrium, which is continuously disturbed by reaction of **4** to **5** and might have a considerable error.

$$\mathbf{3} \underset{k_{-1}}{\overset{k_1}{\rightleftharpoons}} \mathbf{4} \xrightarrow{k_2} \mathbf{5} \tag{4}$$

To identify the palladium species present during catalysis, a 100-fold excess of **3** was added to a solution of **6** in $CDCl_3$ and a $^{31}P\{^1H\}$-NMR spectrum of the mixture taken. The chemical shift of the ^{31}P nuclei is a sensitive probe for processes occurring at the

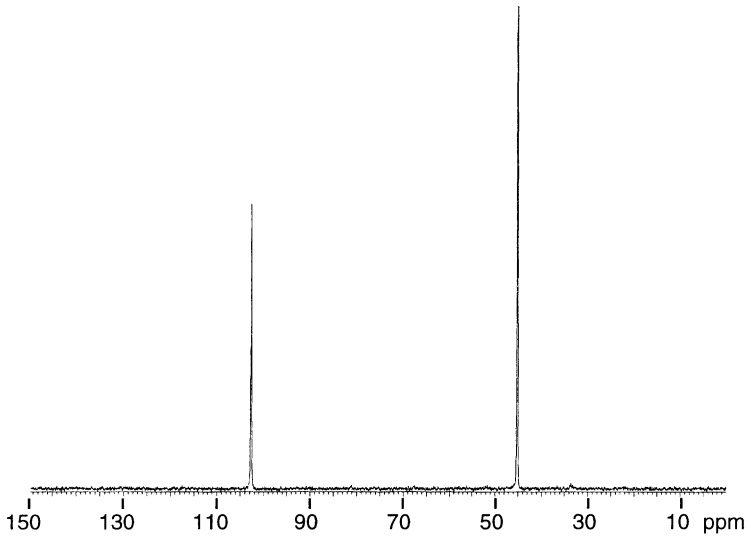

Fig. 4. $^{31}P\{^{1}H\}$-NMR spectrum of the reaction mixture during the cyclisation of **3** with [Pd(Triphos)]$(CF_3SO_3)_2$.

palladium centre. During catalysis, only two signals were detected in the spectra at 102.8 and 45.2 ppm in a ratio of 1:2 (Fig. 4). These can be assigned to the PPh moiety and the two PPh_2 groups of an unknown palladium complex **7**. The high concentration of the complex in the catalytic mixture indicates that **7** is either a resting state of the catalyst or that the subsequent step in the catalytic cycle is a slow reaction.

In order to identify this complex, 1 equivalent (eq.) of 6-aminohex-1-yne was added to a solution of **6** in $CDCl_3$. The $^{31}P\{^{1}H\}$-NMR spectrum of the mixture showed two signals at 109.5 and 53.9 ppm in a 1:2 ratio. These can be assigned to formation of the cyclisation product **5**, which remains coordinated to the palladium centre (giving complex **9**). Additional weaker signals at 116.7/52.7 and 102.7/45.2 ppm can be assigned to the parent palladium complex **6** and the unknown intermediate **7**, respectively (Table 1). It is known that amines can attack alkynes, which are coordinated to a late transition metal centre [17,18]. To test the hypothesis that **7** is the result of a corresponding nucleophilic attack, 1 eq. heptyne and 1 eq. NEt_3 were added in succession to a solution of **6**. Complex **8** formed in situ, according to Eq. (5), and gave rise to two signals in the $^{31}P\{^{1}H\}$-NMR spectrum, which occur at exactly the same chemical shift

Table 1
$^{31}P\{^{1}H\}$-NMR signals observed for in situ mixtures of [Pd(Triphos)]$(CF_3SO_3)_2$ and various ligands

Ligand for [Pd(Triphos)]$(CF_3SO_3)_2$	δ(P1) (ppm)	δ(P2/3) (ppm)	Concentration (%)	Assignment
$HC{\equiv}C(CH_2)_4NH_2$ (1 eq.) (**3**)	116.7	52.7	2	**6**
	109.5	53.9	90	**9**
	102.7	45.2	8	**7**
$HC{\equiv}C(CH_2)_4NH_2$ (100 eq.) (**3**)	102.8[a]	45.2[a]	100	**7**
(1) $HC{\equiv}C(CH_2)_4CH_3$ (1 eq.)	116.7	52.5	4	**6**
(2) NEt_3 (1 eq.)	112.7	47.5	5	**10**[b]
	102.9	45.3	91	**8**

[a] 102.8 t ($J(^{31}P, ^{31}P) = 17.7$ Hz); 45.2 d ($J(^{31}P, ^{31}P) = 17.8$ Hz).
[b] Complex **10**: [Pd(Triphos)(NEt_3)]$(CF_3SO_3)_2$.

as observed for the unknown intermediate **7**. Thus, the direct environment of the palladium centre must be very similar in complexes **7** and **8** and is assigned to $[(\text{Triphos})Pd^{2+} \leftarrow CH^{-}{=}CR{-}NR'_3{}^{+}]$ with R = alkyl, R′ = H/alkyl (Eqs. (5) and (6)). Thus, it seems likely that complex **7** has formed by nucleophilic attack of the amine on the coordinated alkyne.

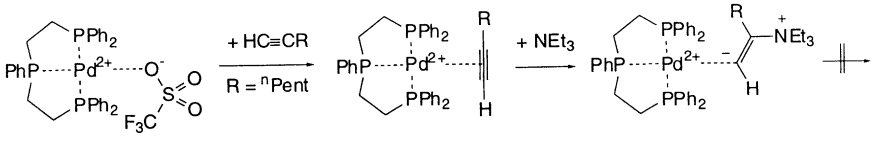

(5)

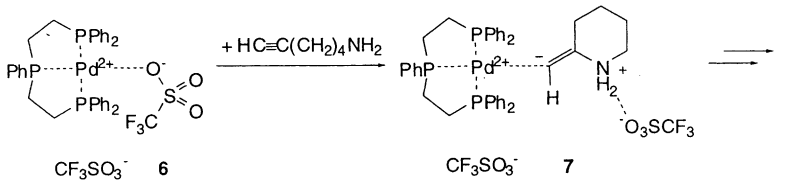

(6)

Zinc was chosen for the preparation of the corresponding heterogeneous catalysts. It has only one oxidation state available, which allows for a more straightforward mechanistic analysis. The catalysts were prepared by ion exchanging H-beta zeolite with zinc acetate, followed by calcination at 450 °C [19]. The Zn–H-beta zeolites, with zinc concentrations between 0.03 and 0.66 mmol Zn^{2+}/g, were tested as catalysts in the cyclisation of **3**. The solvent toluene was chosen, as higher reaction rates were obtained than for more polar solvents, such as acetonitrile. The initial rate of cyclisation varied from 1.7×10^{-3} to 6.0×10^{-2} mol $(g_{cat}\ h)^{-1}$ (111 °C). At low zinc content, the reaction rate increased linearly with the zinc concentration (Fig. 5). Above a zinc concentration of 0.31 mmol Zn^{2+}/g, however, the catalytic activities of the Zn–H-beta zeolites remained constant. The additional, catalytically inactive, zinc could be present in the zeolite pores as ZnO, which does not contribute to the catalytic activity.

Interestingly, the amount of ammonia which adsorbed on the Zn–H-beta zeolites correlated

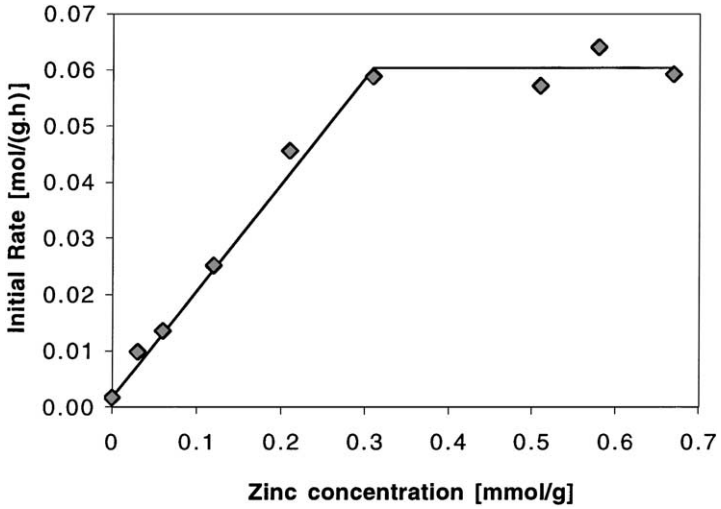

Fig. 5. Catalytic activity of Zn–H-beta zeolites in the cyclisation of **3** (solvent toluene, 111 °C).

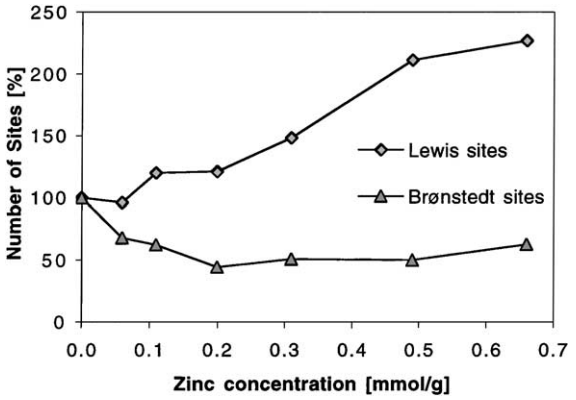

Fig. 6. Semi-quantitative determination of the number of Brønsted and Lewis acid sites by pyridine adsorption and IR spectroscopy. The number of sites is given relative to the number of sites in the parent H-beta catalyst.

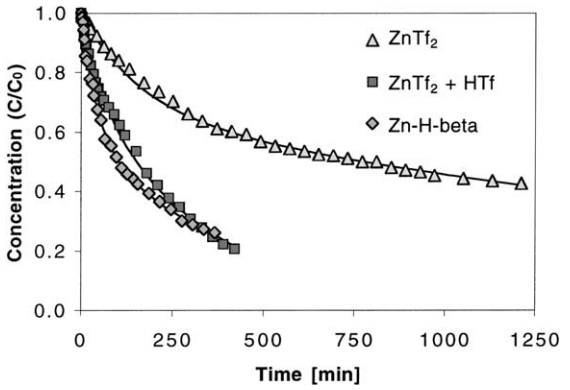

Fig. 7. Comparison of the cyclisation of **3** with homogeneous ($Zn(CF_3SO_3)_2$) and heterogeneous catalysts (Zn–H-beta, 0.51 mmol Zn^{2+}/g); Tf^- denotes $CF_3SO_3^-$. The reactions were performed in toluene at 111 °C and the concentrations followed *on line* with NIR spectroscopy.

with the catalytic activity of the materials [20]. The parent H-beta adsorbed 0.46 mmol NH_3/g. The amount of ammonia adsorbed increased linearly with the zinc content to 0.66 mmol NH_3/g. Above 0.31 mmol Zn^{2+}/g the amount of ammonia adsorbed remained approximately constant. This shows that the catalytically inactive ZnO species do not adsorb ammonia.

Semi-quantitative evaluation of the number of Brønsted and Lewis acid sites was possible by pyridine adsorption and IR spectroscopy [21]. A band at 1546 cm^{-1}, assigned to the CC stretch vibration of pyridine, is characteristic for pyridine adsorbed on Brønsted acid sites, whereas a band at 1451 cm^{-1} is due to pyridine molecules adsorbed on Lewis sites [22]. From the intensity of the signals the number of Brønsted and Lewis sites in the material could be estimated relative to the parent H-beta zeolite (Fig. 6). The number of Lewis sites increased continuously with the zinc content. The number of Brønsted acid sites decreased at low zinc concentrations, whereas above 0.21 mmol Zn^{2+}/g the number remained approximately constant. About half of the protons initially present in H-beta could not be exchanged by zinc cations.

To compare corresponding homogeneous and heterogeneous catalysts, the zinc salt $Zn(CF_3SO_3)_2$ and Zn–H-beta (0.51 mmol Zn^{2+}/g) were tested as catalysts in the cyclisation of **3** (toluene, 111 °C) [14]. Under the same reaction conditions Zn–H-beta had a higher catalytic activity than the corresponding homogeneous catalyst $Zn(CF_3SO_3)_2$ (Fig. 7). It seemed likely that the protons remaining in the beta zeolite after the ion exchange could function as a co-catalyst. To test this hypothesis, CF_3SO_3H (20 equivalents relative to Zn^{2+}) was added to a catalytic mixture of $Zn(CF_3SO_3)_2$ and **3**. The catalytic activity of $Zn(CF_3SO_3)_2$ increased to such an extend that it was similar to the Zn–H-beta zeolite. In contrast, acid without a metal catalyst did not lead to a conversion of **3**. Fitting of the kinetic model showed that, after addition of CF_3SO_3H, k_1 and k_{-1} increased by a factor of 4 and k_2 by 25. This indicates that the protons function as co-catalysts in the cyclisation of **3**–**5** by accelerating the hydroamination as well as the isomerisation of the enamine to the imine. Thus, we postulate that a proton transfer step is involved in both elementary steps.

The addition of amine N–H to CC unsaturated bonds seemed best catalysed with a catalytic system comprising Lewis and Brønsted acidic functionality. To explore this concept, Lewis acidic metal complexes were tested for their catalytic activity in the cyclisation of **1** and **3** (toluene, 111 °C). In particular, the metal complexes $[Rh(NOR)_2]ClO_4$ (NOR = norbornadiene), $Zn(CF_3SO_3)_2$ and $[Cu(CH_3CN)_4]PF_6$ were chosen. Each of the three complexes catalysed the cyclisation of **3**–**5**, although the catalytic

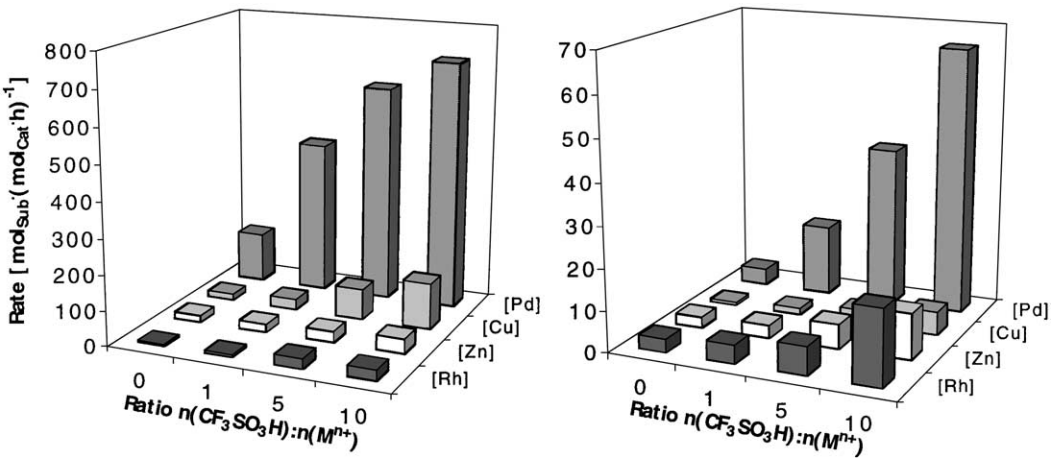

Fig. 8. Initial reaction rates for the cyclisation of **3** (left) and **1** (right) using the catalysts [Pd(Triphos)]$(CF_3SO_3)_2$, [Rh(NOR)$_2$]ClO_4, $Zn(CF_3SO_3)_2$ and [Cu$(CH_3CN)_4$]PF_6 in the presence of different amounts of CF_3SO_3H (solvent toluene, 111 °C).

activity was lower than for [Pd(Triphos)]$(CF_3SO_3)_2$. The same metal complexes also catalyse the cyclisation of **1**–**2**. In each reaction, the addition of a Brønsted acid (CF_3SO_3H) as co-catalyst strongly increased the rate of reaction (Fig. 8).

The similar behaviour of the different catalytic systems indicates a closely related reaction mechanism. A likely reaction sequence for the cyclisation of **3** is shown in Scheme 1. Initially, the substrate coordinates to the palladium centre via the amine lone pair. The complex isomerises so that the alkyne group becomes coordinated to the metal centre. This renders the π-system susceptible to a nucleophilic attack of the nitrogen lone pair, which yields an amphoteric

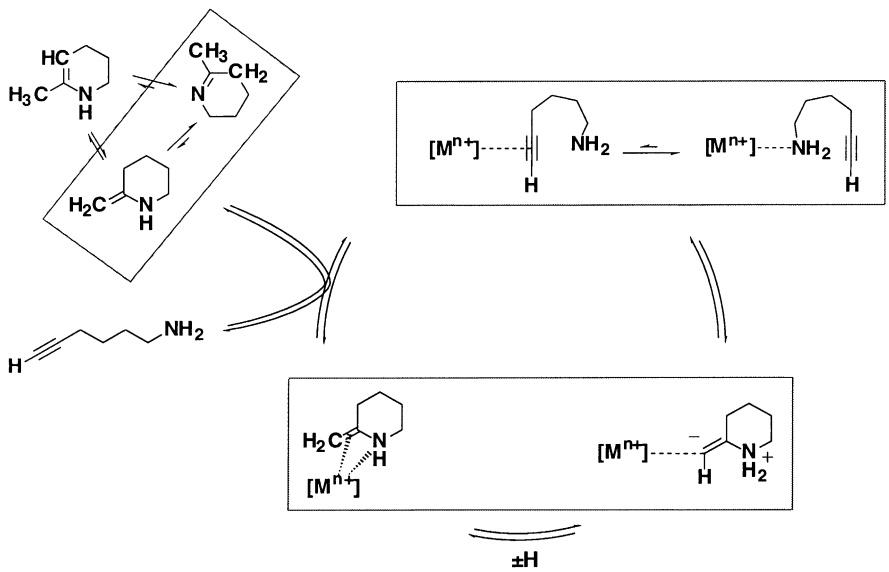

Scheme 1. Reaction sequence proposed for the cyclisation of **3**. The squares indicate those elementary steps where protons are involved.

2-ammonio alken-1-yl complex. Protolytic cleavage of the metal–carbon bond leads to desorption of **4** and regenerates the catalyst. Subsequently, the enamine **4** isomerises in situ to the more stable imine **5**. For the cyclisation of **1**, a corresponding mechanism seems likely except that there is no subsequent isomerisation of the oxazoline formed. Protons are involved in three elementary steps: (A) coordination of the vinylic (**1**) or acetylenic group (**3**) to the metal centre is more likely in acidic conditions as the amine group is protonated reversibly; (B) the intermediate amphoteric complex rearranges by a formal 1,3-proton shift and (C) for the cyclisation of **3**, the isomerisation of the enamine to the corresponding imine is catalysed by protons. The latter could increase the overall reaction rate if the desorption of the intermediate **4** is slow.

4. Conclusions

Lewis acidic complexes of late transition metals were identified as suitable catalysts for the direct addition of amines to CC multiple bonds. This was shown for the cyclisation of 3-aminopropyl-vinylether (**1**) and 6-aminohex-1-yne (**3**). In particular, the complexes $[Rh(NOR)_2]ClO_4$, $[Pd(Triphos)](CF_3SO_3)_2$, $[Cu(CH_3CN)_4]PF_6$ and $Zn(CF_3SO_3)_2$ were active as homogeneous catalysts. Of these complexes, the palladium complex showed the highest catalytic activity in both reactions. The rate of reaction could be increased considerably by the addition of trifluorosulfonic acid as co-catalyst. Although different for the two substrates, the relative order in the activity of the catalysts remained unchanged in acidic reaction conditions.

In contrast to what was expected, the heterogeneous catalyst Zn–H-beta zeolite was catalytically more active than $Zn(CF_3SO_3)_2$. Similar to the homogeneous case, this can be explained by the presence of residual protons in the zinc ion exchanged zeolite. In this respect, it was shown that a maximum of half of the protons in H-beta were exchanged with zinc cations by ion exchange. Thus, Zn–H-beta zeolite is a bifunctional catalyst containing Lewis acidic zinc centres and Brønsted centres in close vicinity.

The similarities between homogenous and heterogeneous catalysts indicate that the reaction mechanism is also similar. Several techniques were employed to obtain data on the elementary steps of the reaction. $^{31}P\{^1H\}$-NMR spectroscopy was used to investigate which metal complexes occur during the cyclisation of **3** with the homogenous catalyst $[Pd(Triphos)](CF_3SO_3)_2$. It was shown that the predominant metal species in the catalytic mixture is the result of a nucleophilic attack of the amine on a coordinated alkyne. The high concentration of the complex indicates that the subsequent step, protolytic cleavage of the metal–carbon bond in the intermediate complex, is a slow step in the mechanistic cycle. This step probably occurs faster in acidic conditions. However, two further steps were identified where protons are involved in the reaction cycle. In summary, these results show that Brønsted and Lewis acidic groups in close vicinity may be necessary in an ideal catalyst for hydroamination reactions.

Acknowledgements

Van Nhu Nguyen is thanked for following the reaction with NIR and UV spectroscopy. Dr. Herdtweck and Manja Grosche are thanked for performing the single crystal X-ray structure analysis. The financial contributions of “DSM”, “Deutsche Forschungsgemeinschaft”, “Stiftung Stipendien-Fonds des Verbandes der Chemischen Industrie e.V.” and “Dr.-Ing. Leonhard-Lorenz-Stiftung” are gratefully acknowledged. Xaver Hecht and Andreas Marx are thanked for the experimental support.

References

[1] K. Tanabe, W.F. Hölderich, Appl. Catal. A 181 (1999) 399.
[2] V. Taglieber, W. Hölderich, R. Kummer, W.D. Mross, G. Saladin, EP Patent 0 132 736 B1 (7 October 1987), to BASF AG.
[3] W. Hölderich, V. Taglieber, H.H. Pohl, R. Kummer, K.G. Baur, EP Patent 0 263 462 B1 (27 November 1991), to BASF AG.
[4] V. Taglieber, W. Hölderich, R. Kummer, W.D. Mross, G. Saladin, EP Patent 0 133 938 B1 (5 November 1986), to BASF AG.
[5] H.F. Koch, L.A. Girard, D.M. Roundhill, Polyhedron 18 (1999) 2275.
[6] T.E. Müller, in: Hydroamination, Section B: Heterogeneous, I.T. Horváth (Ed.), Encyclopedia of Catalysis, Wiley, New York, 2002, in press.
[7] A. Chauvel, B. Delmon, W.H. Hölderich, Appl. Catal. 115 (1994) 173.

[8] W. Hölderich, M. Hesse, F. Naumann, Angew. Chem. Int. Ed. Eng. 27 (1988) 226.
[9] T.E. Müller, M. Grosche, E. Herdtweck, A.-K. Pleier, E. Walter, Y.-K. Yan, Organometallics 19 (2000) 170.
[10] N. Van Nhu, A. Wanner, H. Tiltscher, J.A. Lercher, Catal. Today 66 (2001) 335.
[11] T.E. Müller, M. Berger, M. Grosche, E. Herdtweck, F.P. Schmidtchen, Organometallics 20 (2001) 4384.
[12] M. Beller, H. Trauthwein, M. Eichberger, C. Breindl, T.E. Müller, Eur. J. Inorg. Chem. (1999) 1121.
[13] M. Beller, H. Trauthwein, M. Eichberger, C. Breindl, J. Herwig, T.E. Müller, O.R. Thiel, Chem. Eur. J. 5 (1999) 1306.
[14] V.N. Nguyen, T.E. Müller, J.A. Lercher, AIChE Journal (2002), submitted for publication.
[15] K.A. Connors, Chemical Kinetics: The Study of Reaction Rates in Solution, VCH, Weinheim, 1990, p. 87.
[16] J.H. Espenson, Chemical Kinetics and Reaction Mechanisms, 2nd Edition, McGraw-Hill, New York, 1995, p. 77 (Chapter 4.3).
[17] B. Akermark, J.-E. Bäckvall, K. Zetterberg, Acta Chem. Scand. B 36 (1982) 577.
[18] J. Ambüehl, P.S. Pregosin, L.M. Venanzi, G. Ughetto, L. Zambonelli, Angew. Chem. Int. Ed. Engl. 44 (1975) 369.
[19] J. Penzien, T.E. Müller, J.A. Lercher, J. Chem. Soc., Chem. Comm. 18 (2000) 1753.
[20] J. Penzien, T.E. Müller, J.A. Lercher, Micropor. Mesopor. Mater. 48 (2001) 285.
[21] T.E. Müller, J. Penzien, J.A. Lercher, J. Am. Chem. Soc. (2002), manuscript.
[22] C.E. Emeis, J. Catal. 141 (1993) 347.